

# Growth of Phosphate Coating on Titanium Substrate by Hydrothermal Process

Yao-Shan Hsu,<sup>a</sup> Edward Chang<sup>a</sup> & Hok-Shin Liu<sup>b</sup>

<sup>a</sup>Department of Material Engineering, National Cheng Kung University, Tainan 701, Taiwan, ROC

<sup>b</sup>Department of Resources Engineering, National Cheng Kung University, Tainan 701, Taiwan, ROC

(Received 6 March 1996; accepted 26 June 1996)

**Abstract:** A modified hydrothermal process was utilized to deposit phosphates on titanium alloy substrate by a nucleation and growth mechanism. Reagent grade hydroxyapatite powder and CaO and P<sub>2</sub>O<sub>5</sub> powders were used as raw materials, and deionized water with or without phosphoric acid as reaction media. It was found that phosphates of CaTi<sub>4</sub>(PO<sub>4</sub>)<sub>6</sub> phase and an unknown phase were deposited on the titanium substrate when phosphoric acid was added in the deionized water, with CaO and P<sub>2</sub>O<sub>5</sub> as the reaction powders. The CaTi<sub>4</sub>(PO<sub>4</sub>)<sub>6</sub> phase and the unknown phase were apparently formed by the mechanism of nucleation and growth, with the former phase acting as the bonding under-layer and the latter as the top layer grown on to the under-layer. © 1997 Elsevier Science Limited and Techna S.r.l.

## 1 INTRODUCTION

Ceramics such as silicates, oxides, carbides, borides and nitrides, silicides, etc., are used as coating materials on metal substrates for applications requiring biocompatibility, dielectric property, corrosion, high temperature and wear resistances.<sup>1</sup> Various methods, such as physical vapour deposition (PVD),<sup>2,3</sup> chemical vapour deposition (CVD),<sup>4,5</sup> spraying,<sup>1</sup> electrophoresis<sup>6,7</sup> and plasma spraying,<sup>8,9</sup> are used to join the ceramics to the metals. Each method has its advantages and limitations. The bonding between ceramics and metals by the PVD process is usually poor and the coating is usually limited to a thin film. The bonding can be improved by the CVD process, but the coating might spall on cooling from the higher deposition temperature due to the difference in coefficient of thermal expansion between ceramics and metals. The fusionless process of electrophoresis may need sintering or fusion after coating to increase the density and the coating may crack due to the shrinkage of the films and thermal mismatch stress generated between ceramics and metals. For fusion processes like plasma spraying, residual stress,<sup>10</sup> compositional change and phase decomposition may occur.<sup>11</sup> Thus a low tempera-

ture process which could bond a thick layer of ceramic materials to metal substrates would be of technical interest.

Deposition or growth of insoluble single-component oxides on metal surfaces can be achieved by an electrochemical method,<sup>12,13</sup> however, growth of multiple-component ceramics on metal surfaces is seldom reported. Formation of ceramic-like coatings on metals by the methods of nucleation and growth may have the intrinsic advantage of minimum interface energy and good bonding strength. In this preliminary attempt, phosphate materials were deposited on to a titanium substrate by the hydrothermal method. The ultimate goal is to form a hydroxyapatite coating on metal surfaces. Previously, Hattori *et al.*<sup>14,15</sup> used Ca<sub>2</sub>P<sub>2</sub>O<sub>7</sub> and CaO as raw materials to prepare hydroxyapatite powders under hydrothermal conditions. After 3 h at 350°C and 30 MPa, hydroxyapatite powders were synthesized. At 473°C and 70 MPa, transformation of Ca<sub>2</sub>P<sub>2</sub>O<sub>7</sub>, CaO and H<sub>2</sub>O into hydroxyapatite powders was completed within 1 h; when only Ca<sub>2</sub>P<sub>2</sub>O<sub>7</sub> and H<sub>2</sub>O were used as raw materials at 500°C and 80 MPa, hydroxyapatite powders were detected after 96 h. Despite the success in synthesizing powders, the method and conditions to deposit and grow multiple-component ceramic-

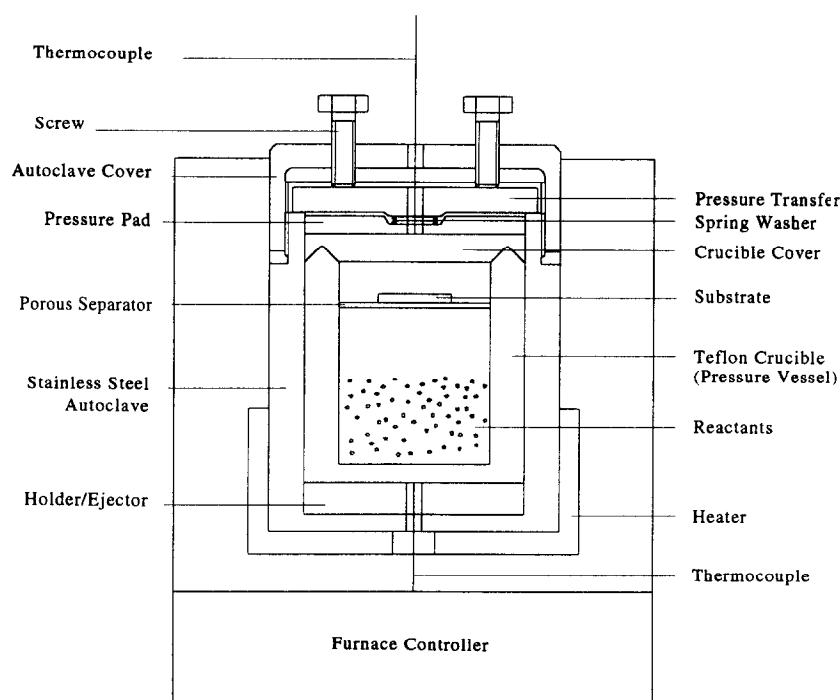


Fig. 1. The experimental apparatus and specimen arrangement for hydrothermal reactions.

like coatings on to metal substrates hydrothermally might be more involved.

## 2 EXPERIMENTAL PROCEDURE

Figure 1 shows the experimental apparatus in which the specimen and reactants were contained — a Teflon crucible with an empty volume of 10 ml encapsulated in a stainless steel autoclave. The heater was placed below the autoclave and the top of the stainless steel autoclave was naturally cooled. Thermocouples were placed at the bottom and top of the teflon crucible. From measurement,

a thermal gradient of approximately 22°C/cm was recorded between the bottom and top position of the autoclave for a heater temperature between 200 and 300°C. The purpose of placing the specimens at a distance above the reactants was to induce a convective flow that will bring the reactants to the surface of the substrate.

Ti-6Al-4V plates (RMI HT 852214-03-00GA 045) were used as the substrate material. The plates were cut into 20 mm×20 mm×1 mm samples, polished by #240, #320, #600 and #1200 emery cloths, and then ultrasonically cleaned in acetone and deionized water. The experimental conditions of hydrothermal reactions are shown in Table 1. As

Table 1. The experimental conditions of hydrothermal reactions

Specimen no.	Ti-6Al-4V substrate	Reaction powders (g) and media (ml)		Reaction temperature (°C)	Reaction time (h)
1	As-polished	—		—	—
2	As-polished	HA	1.00	300	24
		H <sub>2</sub> O	1.00		
3	As-polished	CaO	1.32	300	24
		P <sub>2</sub> O <sub>5</sub>	1.00		
		H <sub>2</sub> O	0.50		
4	Immersed in H <sub>3</sub> PO <sub>4</sub> ×24 h <sup>a</sup>	HA	1.00	300	24
		H <sub>2</sub> O	0.50		
5	As-polished	CaO	1.32	300	24
		P <sub>2</sub> O <sub>5</sub>	1.00		
		H <sub>2</sub> O	0.50		
		H <sub>3</sub> PO <sub>4</sub>	1.80		

<sup>a</sup>Prior to hydrothermal reaction.

shown in this table, specimen 1 was the as-polished Ti-6Al-4V substrate. Specimens 2 and 3 were processed hydrothermally in the crucible containing reactants of HA (hydroxyapatite, Merck, pure reagent grade) plus deionized water, and CaO (Nihon Shiyaku Industries Ltd, extra pure reagent grade),  $P_2O_5$  (First Chemicals Ltd, reagent chemical grade) plus deionized water, respectively. For specimen 4, the polished substrate was pre-treated in  $H_3PO_4$  for 24 h before being placed in the crucible with powders and media of HA and deionized water. The phosphoric acid solution was prepared by adding 20 ml  $H_3PO_4$  (Nihon Shiyaku Industries Ltd, extra pure reagent grade) into 20 ml deionized water. Alternatively,  $H_3PO_4$  was added to CaO,  $P_2O_5$  and deionized water for the hydrothermal reaction of specimen 5. Using the cylindrical teflon crucible contained in the stainless steel autoclave as shown in Fig. 1, the raw materials and reaction media were hydrothermally reacted at the nominal temperature of 300°C, measured from the bottom of crucible, for 24 h. After hydrothermal reaction, the specimens were taken out to investigate the phases and microstructure of the hydrothermal reaction products by the techniques of X-ray diffraction (Siemens D 5000) with  $CuK_{\alpha}$  radiation and scanning electron microscopy (ABT-55). The chemical compositions of the growth

products were analysed by energy dispersive spectroscopy (EDS).

### 3 RESULTS AND DISCUSSION

The results of XRD patterns for specimens 1–4 are shown in Fig. 2, in which Fig. 2(a), (b), (c) and (d) correspond to specimens 1, 2, 3 and 4, respectively. In Fig. 2(a), the peaks emit obviously from the reflections of the titanium alloy. Little difference in the XRD patterns between specimens 2–4 and specimen 1 is revealed, and these results imply that few, if any, reaction products were generated in specimens 2–4. Some specimens not mentioned in Table 1 were directly immersed in the reactants instead of being kept at a distance from the media as shown in Fig. 1, yet the reactants could not be adhered to the metal surfaces. Additionally, a thin film X-ray diffractometer (Philip PW 1729) was used to detect any possible thin oxides on the metal surface of specimen 2, but similar results to Fig. 1 were found, except for a higher background intensity at low  $2\theta$  angles.

The SEM morphology of specimen 5 — grown with the powders and media of CaO,  $P_2O_5$ ,  $H_2O$  and  $H_3PO_4$  — is shown in Fig. 3(a). The thickness of the grown layers after reaction at 300°C for 24 h

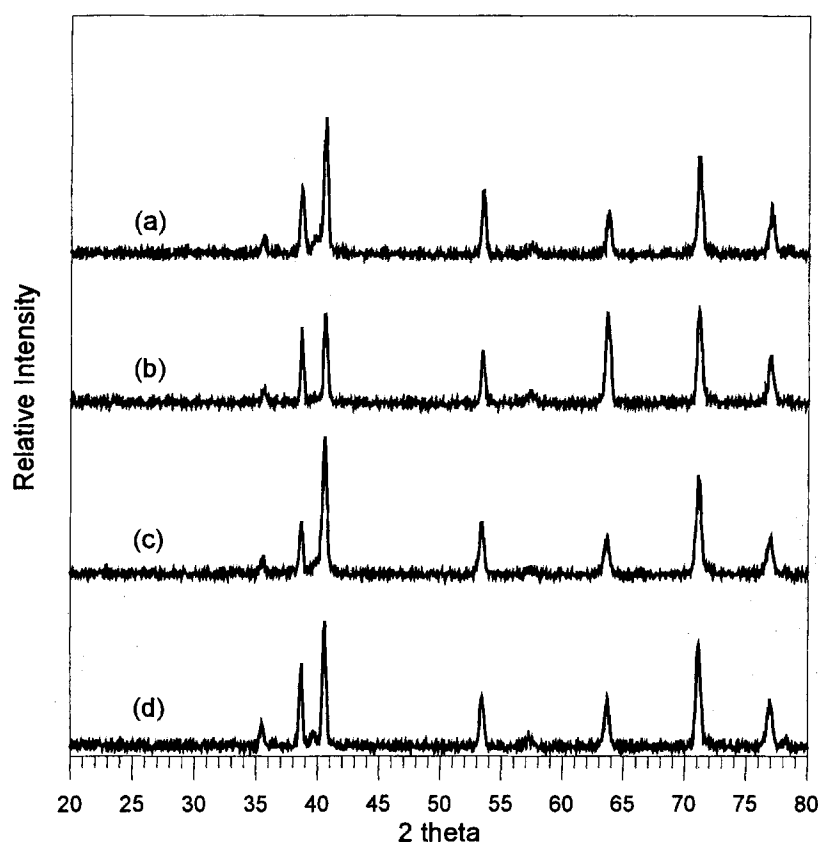


Fig. 2. The XRD patterns of specimens (a) 1, (b) 2, (c) 3 and (d) 4 described in Table 1.



Fig. 3. The SEM morphology of specimen 5 reacted hydrothermally at 300°C for 24 h using CaO and P<sub>2</sub>O<sub>5</sub> powders with deionized water and phosphoric acid as reaction media: (a) darker under-layer and lighter upper layer (the arrow is explained in the text); (b) upper layer at higher magnification.

is about 0.5 mm. Observation of Fig. 3(a) reveals that the grown products consist of two distinctive layers, namely, an under-layer and a top layer; the under-layer possesses a darker contrast under SEM

and the top layer possesses a lighter contrast. Apparently, the darker under-layer grew first on the titanium substrate, and the lighter top layer nucleated and grew on the under-layer. It is interesting to see that the top layer was invading the under-layer as shown by the direction of the arrow in Fig. 3(a). The local feature of the top layer at higher magnification is shown in Fig. 3(b).

Observation of Fig. 3 reveals that, apparently, both the under-layer and the top layer consist of a respective single phase, i.e. a mixture of more than one phase in either the under-layer or the top layer is not apparent. The result of X-ray diffraction pattern of the scratched powders from specimen 5 is shown in Fig. 4. Examination of the peaks leads to the conclusion that one of the phases corresponding to the strongest peak and others in Fig. 4 can be identified as the CaTi<sub>4</sub>(PO<sub>4</sub>)<sub>6</sub> phase (abbreviated as T4 phase) (JCPDS 35-740), but other major peaks, as labelled by circles in this figure, can not be attributed to the reflection from the T4 phase. It is very difficult to match the circled reflections with the JCPDS sets 1–45. Oxides such as Ti<sub>9</sub>O<sub>17</sub> (JCPDS 18-1405) and Ca<sub>3</sub>Ti<sub>2</sub>O<sub>7</sub> (JCPDS 14-151) did not fit the circled unknown phase. Several phases containing elements Ti, H, P and O, such as Ti(HPO<sub>4</sub>)<sub>2</sub> (JCPDS 33-1377) and Ti(HPO<sub>4</sub>)<sub>2</sub>·H<sub>2</sub>O (JCPDS 33-1378 and 33-1379), also did not fit. Other attempts to search for phases containing elements Ca, H, P and O, such as Ca<sub>3</sub>(PO<sub>4</sub>)<sub>2</sub> (JCPDS 29-359), Ca<sub>3</sub>(PO<sub>4</sub>)<sub>2</sub>·nH<sub>2</sub>O (JCPDS 18-303), Ca<sub>1.5</sub>HP<sub>2</sub>O<sub>7</sub>·2H<sub>2</sub>O (JCPDS 12-28), Ca<sub>10</sub>(PO<sub>4</sub>)<sub>6</sub>(OH)<sub>2</sub> (JCPDS 9-432), CaHPO<sub>4</sub> (JCPDS 9-80) and CaHPO<sub>4</sub>·2H<sub>2</sub>O (JCPDS 7-77), failed to unambiguously identify the circled unknown phase. Moreover, the reaction powders of CaO (JCPDS 28-775), Ca(OH)<sub>2</sub> (JCPDS 4-733)

Table 2. EDS analysis of the chemical composition of the under-layer

Element	ZAF <sup>a</sup>	Wt%	At.%	At.% <sup>b</sup>	Atomic Ca/Ti ratio
Ca K <sub>α</sub>	1.010	9.905	8.833	8.880	—
Ti K <sub>α</sub>	0.861	31.548	23.540	23.666	—
Al K <sub>α</sub>	0.990	0.400	0.530	—	—
P K <sub>α</sub>	1.343	58.138	67.096	67.454	—
Total	—	99.991	100.00	100.00	0.38

<sup>a</sup>Correction factor by internal standard.

<sup>b</sup>Neglecting Al.

Table 3. EDS analysis of the chemical composition of the upper layer

Element	ZAF <sup>a</sup>	Wt%	At.%	At.% <sup>b</sup>	Atomic Ca/Ti ratio
Ca K <sub>α</sub>	0.992	27.589	24.115	24.151	—
Ti K <sub>α</sub>	0.824	15.113	11.053	11.069	—
Al K <sub>α</sub>	0.993	0.113	0.147	—	—
P K <sub>α</sub>	1.341	57.183	64.685	64.780	—
Total	—	99.998	100.00	100.00	2.17

<sup>a</sup>Correction factor by internal standard.

<sup>b</sup>Neglecting Al.

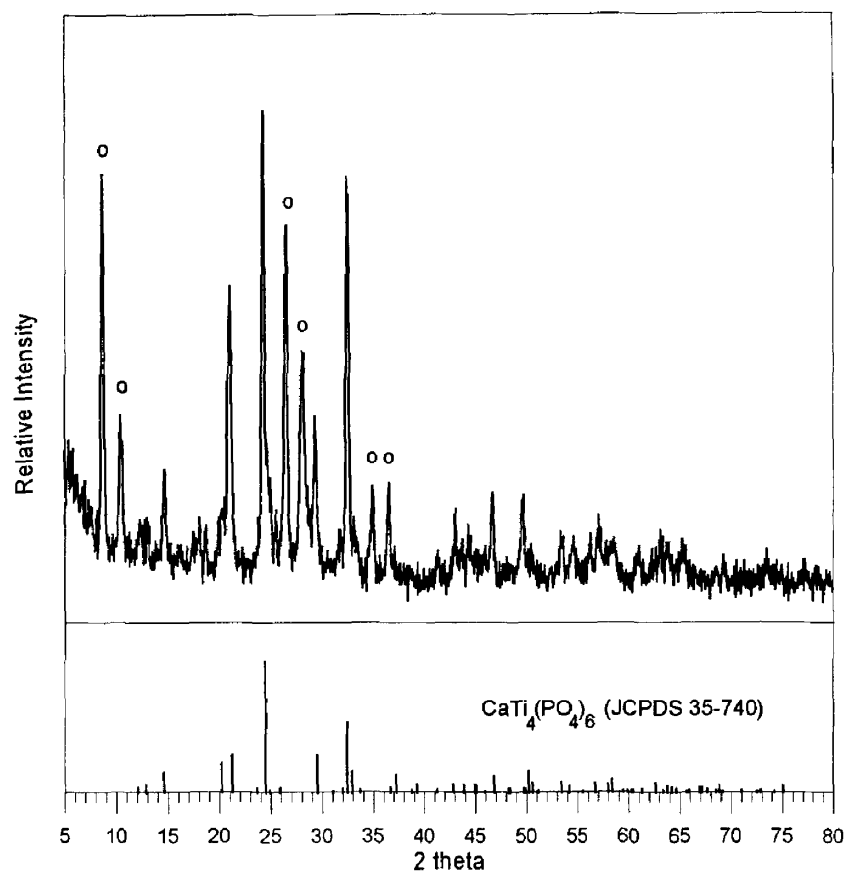


Fig. 4. The XRD patterns of specimen 5 and the mating  $\text{CaTi}_4(\text{PO}_4)_6$  phase. (○ denotes the major peaks not fitted by the  $\text{CaTi}_4(\text{PO}_4)_6$  phase).

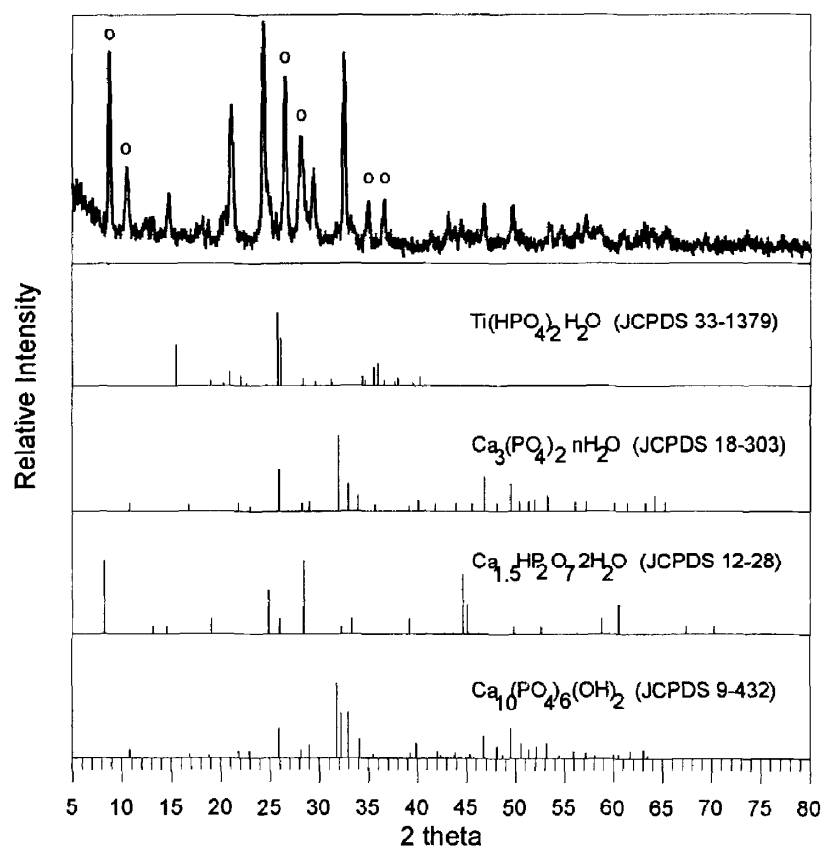


Fig. 5. Fitting of an unknown phase by several phases from JCPDS sets 1-45.

and  $P_2O_5$  (JCPDS 5-318 and 4-733) were suspected to coat the titanium substrate directly, and yet the fits were poorer. Part of the efforts of fitting are shown in Fig. 5. Attempts considering elements Ca, H, Ti, P and O were also made, but the JCPDS sets 1–45 contained only one relevant phase and this phase is  $CaTi_4(PO_4)_6$ .

It is also unknown as to what layer in Fig. 3 corresponds to the T4 phase in Fig. 4. The EDS analysis of chemical compositions from the under-layer and the top layer in Fig. 3 are shown in Tables 2 and 3, respectively. Both layers contain the elements Ca, Ti and P, but the under-layer contains less calcium relative to titanium. The under-layer possesses an atomic Ca/Ti ratio of 0.38 (internal standard calibration, Table 2) and the top layer possesses a ratio of 2.17 (Table 3). As both layers possess a respective single layer, it is deduced that the under-layer should correspond to the T4 phase since this phase possesses a ratio of 0.25, which is closer to the ratio of the under-layer. Assuming this is correct and taking the T4 phase as the external standard to calibrate the chemical compositions in Table 2, the calibrated factors can be obtained to estimate the corrected chemical composition of the top layer. It is estimated that the formula of the top layer is close to  $Ca_2Ti(PO_4)_4$  or  $Ca_2Ti(HPO_4)_4$ ; for the latter phase the balance of valance has been taken into consideration. The mechanism of phosphate bonding in ceramics has been reported in the literature.<sup>16</sup> For the present T4 phase, the possibility of a titanium atom joining with a titanium substrate and the availability of calcium and phosphorus atoms to join with calcium phosphates suggests that the material warrants further study to promote the bonding of titanium alloy with calcium phosphate ceramics.

## 4 CONCLUSION

A modified hydrothermal process was developed that enabled ceramic-like coatings to be deposited on a titanium alloy substrate. The experimental results are summarized as follows:

- (1) When phosphoric acid was added in the deionized water using CaO and  $P_2O_5$  as the reaction powders, phosphates of  $CaTi_4(PO_4)_6$  phase and an unknown phase can be deposited on the titanium alloy substrate.
- (2) The  $CaTi_4(PO_4)_6$  phase and the unknown phase apparently formed by the mechanism of

nucleation and growth, with the former phase nucleated first and joined to the titanium alloy substrate, and the unknown phase then growing on to the  $CaTi_4(PO_4)_6$  phase.

- (3) The unknown phase contained the elements Ca, Ti and P with an approximate atomic Ca/Ti ratio of 2.17, which can not be identified in JCPDS sets 1–45.

## REFERENCES

1. *Surface Cleaning, Finishing and Coating. Metals Handbook*, 9th edn. ASM International, Materials Park, OH, 1982.
2. KONIG, W. & KAMMERMEIER, D., New ways towards better exploitation of physical vapour deposition coatings. *Surf. Coat. Technol.*, **54-55** (1992) 470–474.
3. QUAEYHAEGENS, C., KNUYT, G. D., HAEN, J. & STALS, L. M., Experimental study of the growth evolution from random towards a (111) preferential orientation of PVD TiN coatings. *Thin Solid Films*, **258** (1995) 170–173.
4. YEE, K. K., Protective coatings for metals by chemical vapour deposition. *Int. Metals Rev.*, **1** (1978) 19–42.
5. CHENG, H. E., CHIANG, M. J. & HON, M. H., Growth characteristics and properties of TiN coating by chemical vapour deposition. *J. Electrochem. Soc.*, **142**(5) (1995) 1573–1578.
6. DUCHEYNE, P., RAEMDONCK, W. V., HEUGHEBAERT, J. C. & HEUGHEBAERT, M., Structural analysis of hydroxyapatite coatings on titanium. *Biomaterials*, **7**(3) (1986) 97–103.
7. GRECO, V. P., A review of fabrication and properties of electrocomposites. *Plating and Surface Finishing*, **76**(10) (1989) 68–72.
8. WU, B. C., CHANG, E., CHANG, S. F. & TU, D., Degradation mechanism of  $ZrO_2$ –8 wt%  $Y_2O_3$ /Ni–22Cr–10Al–1Y thermal barrier coatings. *J. Am. Ceram. Soc.*, **72**(2) (1989) 212–218.
9. EVAN, A. G., CRUMLEY, G. B. & DEMARAY, R. E., On the mechanical behaviour of brittle coatings and layers. *Oxidation of Metals*, **20**(5-6) (1983) 193–215.
10. JORDAN, D. W. & FABER, K. T., X-ray residual stress analysis of a ceramic thermal barrier coating undergoing thermal cycling. *Thin Solid Films*, **235** (1993) 137–141.
11. HAMAN, J. D., LUCAS, L. C. & CRAWMER, D., Characterization of high velocity oxy-fuel combustion sprayed hydroxyapatite. *Biomaterials*, **16**(3) (1995) 229–237.
12. PHILIPS, R. J., SHANE, M. J. & SWITZER, J. A., Electrochemical and photoelectrochemical deposition of thallium (III) oxide films. *J. Mater. Res.*, **4**(4) (1989) 923–929.
13. FEUERSANGER, A. E., HANGENLOCHER, A. K. & SOLOMON, A. L., Anodic  $TiO_2$  thin films. *J. Electrochem. Soc.*, **111** (1964) 1387.
14. HATTORI, T. & IWADATE, Y., *J. Am. Ceram. Soc.*, **73**(6) (1990) 1803–1805.
15. HATTORI, T., IWADATE, Y. & KATO, T., *J. Mater. Sci. Lett.*, **8** (1989) 305–306.
16. CASSIDY, J. E., Phosphate bonding then and now. *Ceram. Bull.*, **56**(7) (1977) 640–643.